Available online at www.sciencedirect.com
ScienceDirect
International Journal of Mechanical Sciences 49 (2007) 733–740
International Journal of MECHANICAL SCIENCES
www.elsevier.com/locate/ijmecsci

Investigation of design parameters for droplet generators driven by piezoelectric actuators

Yaw-Shen Chen[a], Yu-Lin Huang[a], Chia-Hsin Kuo[a], Shuo-Hung Chang[a,b,*]

[a]*Department of Mechanical Engineering, National Taiwan University, Taipei, Taiwan, ROC*
[b]*MSL, Industrial Technology Research Institute, Hsin Chu, Taiwan, ROC*

Received 26 September 2006; accepted 16 October 2006
Available online 8 December 2006

Abstract

This paper presents a numerical analysis of a drop-on-demand (DOD) piezoelectric (PZT) actuated droplet generator. A finite difference numerical model was established to analyze the design parameters of droplet ejection. First, we discussed the influence of the driving conditions on the droplet ejection characteristics, such as the driving time and the driving volume change in the pressure chamber. The volume factor, an important design parameter, was proposed from the analysis. The ejected droplets can maintain the same ejection velocity at different nozzle diameters, as long as the volume factor remains the same. Two empirical formulas, based on the analysis data, are suitable for the design of PZT actuated droplet generator. The first empirical formula is a linear relationship between the droplet velocity and the volume factor with a slope of 0.3422 for different nozzle diameters. The second empirical formula defines the driving volume of PZT and nozzle diameter to eject the desired droplets. The geometrical design parameters of droplet generator, such as the nozzle thickness, the pressure chamber width and depth, as well as the driving conditions of the PZT actuator, are all included in the analysis. The sensitivity of geometrical design parameters which affect the droplet volume, the droplet velocity, and the lowest driving condition is established. The quantitative criterion for ejection of droplet, liquid jet, and no droplet is presented. The proposed empirical formula and figures provide easy-to-use tool for design of DOD PZT actuated droplet generators.
© 2006 Elsevier Ltd. All rights reserved.

Keywords: Droplet formation; Piezoelectric inkjet printhead; Drop-on-demand

1. Introduction

With the rapid development of drop-on-demand (DOD) ink-jet print head, the print head plays an important role not only in the office printing applications, but also heavily in the leading-edge technology. The ink-jet printing technique provides advantage of non-contact deposition of liquid crystal display (LCD), polyimide alignment layer, chromatic filter, biotechnology [1], drug distributor [2], fuel injector of engine, tin solder of electrical manufacture [3], optical interconnects, switch, lens, waveguide [4], and OLED [5,6]. Percin and Butrus [7] developed a fluid and solid particle ejector, and a photoresist coating technique by piezoelectric (PZT) droplet generator. In most situations, it is desirable to reduce droplet size, to improve droplet repeatability, and to increase operation frequency.

With the rapid growth of applications mentioned above, the need for understanding of DOD droplet generator has drawn strong attention. Fromm [8] studied the effect of pressure histories driving the jets by numerical calculation. Analysis of 2-D (two-dimensional) and 3-D (three-dimensional) modeling of PZT driven inkjet flow was conducted [9–11]. Although these studies have provided valuable information for DOD PZT droplet generators, effect of design parameters remains unexplored.

This study investigates the design of the droplet ejection of the PZT actuated droplet generator. The design parameters of the droplet generator, such as nozzle diameter (D), nozzle plate thickness (D_t), chamber depth (H) and width (W), as well as the driving condition, such as

*Corresponding author. Department of Mechanical Engineering, National Taiwan University, Taipei, Taiwan, ROC. Tel.: +886 912037135; fax: +886 223631755.
E-mail addresses: shuochang@itri.org.tw, shchang@ntu.edu.tw (S.-H. Chang).

0020-7403/$ - see front matter © 2006 Elsevier Ltd. All rights reserved.
doi:10.1016/j.ijmecsci.2006.10.004

Nomenclature

A	the position of the PZT which moves away from the chamber, as shown in Fig. 2
D	nozzle diameter, as shown in Fig. 2
D_i	nozzle inlet diameter, as shown in Fig. 2
D_t	nozzle plate thickness, as shown in Fig. 2
F	scale function
H	chamber depth, as shown in Fig. 2
P	pressure
S	a closed surface of the control volume
S_d	droplet velocity
S_M	the source term in momentum equation
$\vec{v}$	flow velocity vector
V	driving volume change in the chamber due to PZT displacement
V_A	operating voltage that let the PZT move away from the chamber to the position A
V_d	droplet volume
V_L	the lowest driving volume change
V_S	the control volume bounded by a closed surface S
W	chamber width, as shown in Fig. 2
$\vec{n}$	normal vector in the closed surface S
t	time
t_1	suction time, as shown in Fig. 3
t_2	driving time, as shown in Fig. 3
t_3	resting time, as shown in Fig. 3
ρ	fluid density
$\vec{\tau}$	fluid viscosity tensor
V/D^2	the volume factor

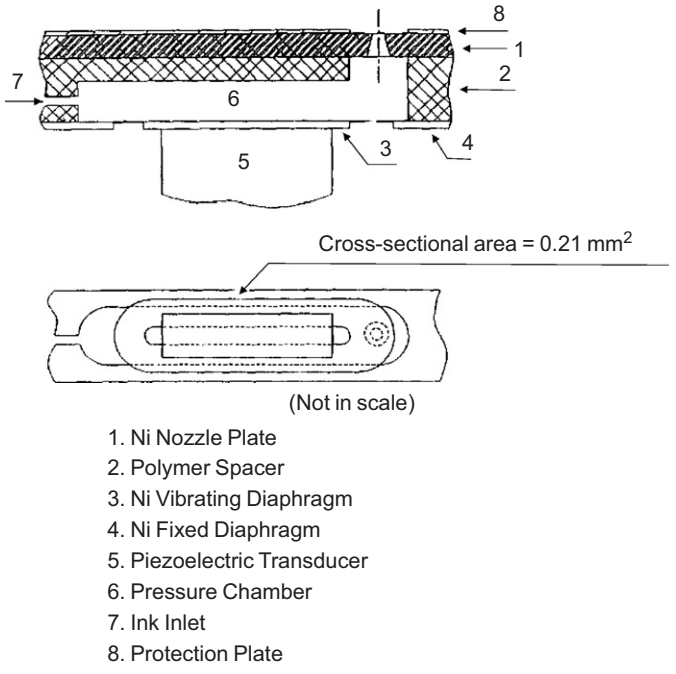

Fig. 1. Schematic view of a commercial PZT print head (not to scale).

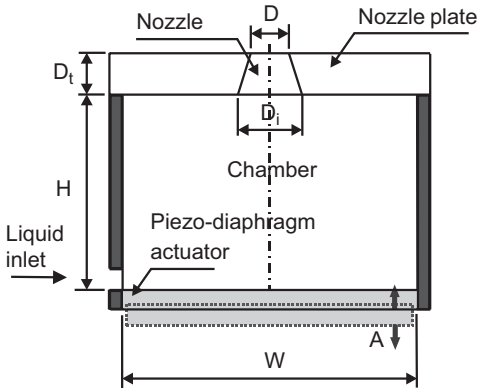

Fig. 2. A 2-D axisymmetric representation of the commercial PZT printhead (not to scale).

driving time (t_2) and driving volume were all included in the model. The analysis aims at the key performance of the droplet generator, i.e., the droplet volume and droplet velocity. Finally, the design procedure based on the analysis results is discussed.

2. Analysis

A commercial PZT-driven ink-jet print head is shown in Fig. 1. It was used in the previous paper [12] and also in this study. From the top to the bottom, this print head consists of a protection layer, a nozzle plate, a spacer, a pressure chamber (or ink flow channel), a diaphragm, and a PZT transducer. The convergent nozzle has a circular cross-section with the inlet diameter, outlet diameter, and height of 40, 80, and 80 μm, respectively. The space of the pressure chamber (6) from the diaphragm (3) to the nozzle plate (1) is 220 μm. The PZT transducer was epoxy glued to the nickel vibrating diaphragm. Note that the extension (4) of nickel vibrating diaphragm was fixed on the spacer (2). The nickel diaphragm has a flexible thin region, with a thickness of 2 μm to provide a hinge for vibration of diaphragm (3) in response to excitation of PZT (5). The PZT transducer has a rectangular cross-section of 500 μm × 50 μm. Connecting to the PZT transducer (5), the moving portion of the nickel diaphragm (3) has a cross-section area of 0.21 mm^2.

Although the flow motion in the pressure chamber of the commercial PZT print head is 3-D, we adopted a 2-D axisymmetric approach in this study. Thus, a simplified circular tube followed by a convergent nozzle is employed to simulate the ink pressure chamber for the commercial print head, as illustrated in Fig. 2. In this model, the 2-D axisymmetric chamber has the same capacity and depth as

in the commercial print head. The uniform distributed displacement at the surface of the PZT was used as a moving boundary condition. Thus, a moving grid for the volume deformation was employed in the iteration of calculation. The incompressible fluid was assumed and the gravity was neglected in the analysis. The working fluid was water instead of ink. It has a surface tension coefficient of 0.0725 N/m and a dynamic viscosity of 1.28 cP.

In this study, a numerical simulation based on the control volume finite difference approach was conducted. The free surfaces of fluid were tracked by using a volume of fluid (VOF) algorithm [13,14] gathered with the fractional area/volume obstacle representation method, which was incorporated into the Navier–Stokes equations of motion as follows:

$$\int_{V_S} \frac{\partial \rho}{\partial t} \, dV + \int_S \rho(\vec{v} \cdot \vec{n}) \, dS = 0, \tag{1}$$

$$\int_{V_S} \frac{\partial}{\partial t} \rho v \, dV + \int_S \rho v(\vec{v} \cdot \vec{n}) \, dS = \int_S nP \, dS + \int_S \vec{n} \cdot \vec{\tau} \, dS + S_M, \tag{2}$$

where the control volume V_S is bounded by a closed surface S with outward normal vector $\vec{n}$, $\vec{v}$ denotes the flow velocity vector, ρ is the fluid density, t is the time, P is pressure, $\vec{\tau}$ is the fluid viscosity tensor, and S_M is the source term in the momentum equation. Because the surface tension plays a major effect on the driving flow, and the total surface force depends on the area of the liquid–gas interface, the source term is appended in the surface tension.

The gas–liquid interface was determined by a scale function F of the liquid volume fraction inside a computational cell. For VOF method, a fluid fraction scale function F, equal to 1 in fluid regions and 0 in air regions, was used to describe the free surface. The scale function F of the liquid volume fraction was induced from the continuity equation based on the assumption of incompressibility, that is,

$$\frac{\partial F}{\partial t} + \vec{v} \cdot \nabla F = 0, \tag{3}$$

where F moves with the fluid and satisfies the continuity equation. In Eq. (3), the gravitational, viscous, and surface tension effects were explicitly included in the model. This implementation of the VOF method was described by Hirt and Nichols [13]. Together with the geometry definition, boundary and initial conditions, Eqs. (1)–(3) were solved by the finite difference approach. To solve the Navier–Stokes and continuity equations, the SIMPLEC (semi-implicit method for pressure-linked equations, consistent) algorithm coupling the pressure and velocity was used [15].

This study is to analyze the influence of design parameters of a DOD droplet generator and also to identify their sensitivities. The design parameters of droplet generator were mainly divided into two groups: driving conditions and parameters of geometrical dimensions. The cross-section of 2-D axisymmetric model shown in Fig. 2, shows the selected parameters of geometrical dimension such as nozzle diameter (D), nozzle plate thickness (D_t), chamber depth (H) and width (W). Based on the commercial DOD PZT ink-jet print heads which were generally fabricated by MEMS technique, the range of design parameters was selected as shown in Table 1. Fig. 3 shows a typical triangular electrical waveform applied to drive the PZT actuator with time intervals t_1, t_2, and t_3. The time interval t_1 is the suction time in which PZT moves away from the chamber to the position A as shown in Fig. 2, and allows the ink to fill the chamber. The time interval t_2 is the driving time in which the PZT displaces toward the nozzle, thus it generates a pressure surge and ejects droplets. Moreover, the t_3 is the resting time in which the PZT returns to its initial position. The maximum operation frequency of the ink droplets of the print head is equal to $1/(t_1 + t_2 + t_3)$. When the electric voltage is kept at zero V for a period of t_3, the PZT undergoes a damped oscillation before it stops completely. Then the PZT is driven by the electric pulse at the end of t_3 to repeat the droplet ejection. The electrical waveform produces a retraction (at positive voltage) followed by a compression (at negative voltage) in the pressure chamber so as to eject the droplets. Therefore, the driving conditions include the driving volume change (V) and the driving time (t_2). The driving volume change (V) represents the decrease of the chamber volume when PZT actuator moves toward the nozzle. Three key performance of DOD PZT droplet

Table 1
Dimensions used in this paper

	The lowest value (μm)	The highest value (μm)
Nozzle diameter, D	20	60
Nozzle plate thickness, D_t	10	90
Chamber depth, H	100	400
Chamber width, W	200	400

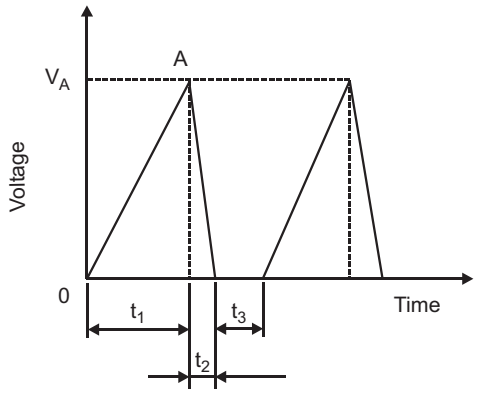

Fig. 3. A typical triangular electrical waveform to drive PZT.

Table 2
Comparison of droplet volume for four different operating conditions between experiment [12] and simulation in this paper

Driving time, t_2 (μs) ($t_1 = 90$ μs, $t_3 = 55$ μs)	Experiment (pl) [12]	Simulation (pl) (this study)	Error (%)
5	45.3	44.3	2.2
7	46.7	47.1	0.8
9	46.3	44.9	3.0
12	39.9	41.8	4.7

generator: droplet velocity (S_d), droplet volume (V_d), and the lowest driving volume change (V_L) were analyzed in this study.

This study adopted the micro-fluid function in the CoventorWare 2003 [14] to calculate the droplet ejection behavior of a DOD droplet generator. It was necessary first to verify the validity. We compared the numerical results with the experimental data in the author's previous work [12]. The initial conditions for Eqs. (1)–(2) were given by $\vec{v} = 0$ and $P = p_0$, where p_0 denotes the initial fluid pressure. The boundary conditions for the nozzle plate and the chamber wall were fixed. The boundary conditions for the PZT was given by $\vec{v} = f(t)$ and $P = p_0$, where $f(t)$ was the time-dependent moving velocity of the PZT when receiving electrical signals. The pressure loss caused by the sudden contraction at the intersection of the circular pipe and the nozzle was neglected. The function $f(t)$ determined by using the ANSYS 5.0A was described in our previous work [12].

To compare our numerical results with previous experimental data [12], the geometrical dimensions were $D = 40\,\mu m$, $D_i = 80\,\mu m$, $D_t = 80\,\mu m$, $H = 300\,\mu m$, and $W = 365\,\mu m$. Under the same driving conditions and geometry dimensions in Ref. [12], the droplet size of the experiment and simulation data was compared in Table 2 for $t_1 = 90\,\mu s$ and $t_3 = 55\,\mu s$. Also, the droplet velocity was compared at driving conditions of $t_1 = 90\,\mu s$ and $t_3 = 55\,\mu s$. When the driving time t_2 was 5 μs (9 μs), the experimental droplet velocity was 10.9 m/s (6.25 m/s). The simulation droplet velocity was 10.2 m/s (6.3 m/s), and the error was 6.2% (0.8%). The errors of 6.2% would be considered acceptable in this study.

3. Results and discussion

3.1. Driving conditions

3.1.1. The lowest and the highest driving conditions

For a droplet generator design, the lowest and the highest driving conditions were identified by the specified driving time (t_2) and the driving volume change (V) which is the change of the chamber volume due to motion of PZT. The lowest driving condition refers to the minimum driving time or driving volume change that was needed to eject a droplet. The highest driving condition refers to the maximum driving time or driving volume change with that the liquid jet instead of droplet will be ejected. In another words, the lowest and the highest driving conditions define the operation region for droplet ejection. Beyond the region, the ejection of droplets becomes impossible. In Fig. 4, the geometrical parameters of $D = 40\,\mu m$, $D_t = 80\,\mu m$, $H = 200\,\mu m$, and $W = 400\,\mu m$, shows the droplet was successfully ejected (a), and not ejected (b) under different driving volume change. By changing the driving time (from 2.5 to 15.0 μs) and nozzle diameter (from 40 to 60 μm in the model), we could find the lowest driving volume change (V_L) to eject a droplet. The results are summarized in Fig. 5. The figure suggests that, the right side region of each line represents the promising operating driving conditions to obtain the droplet ejection. The left side region of each line represents no droplet ejection

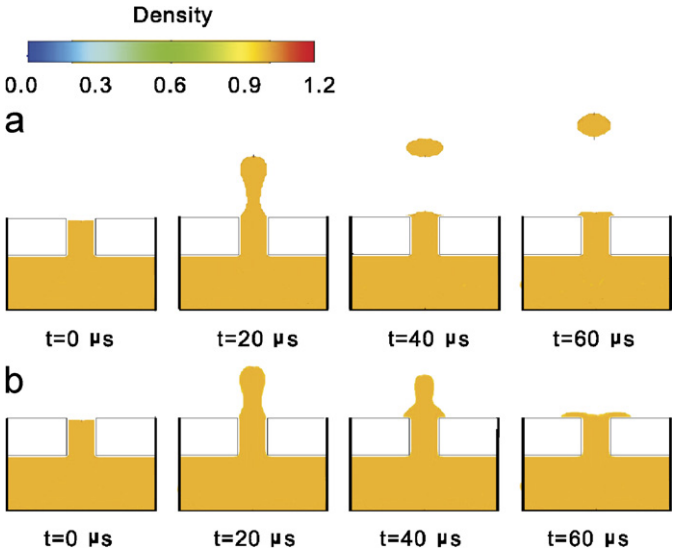

Fig. 4. Simulation results for $D = 40\,\mu m$, $D_t = 80\,\mu m$, $H = 200\,\mu m$, $W = 400\,\mu m$, $t_1 = 90\,\mu s$ and $t_3 = 55\,\mu s$, (a) droplet ejected at $V \geqslant V_d$, (b) droplet not ejected at $V < V_d$.

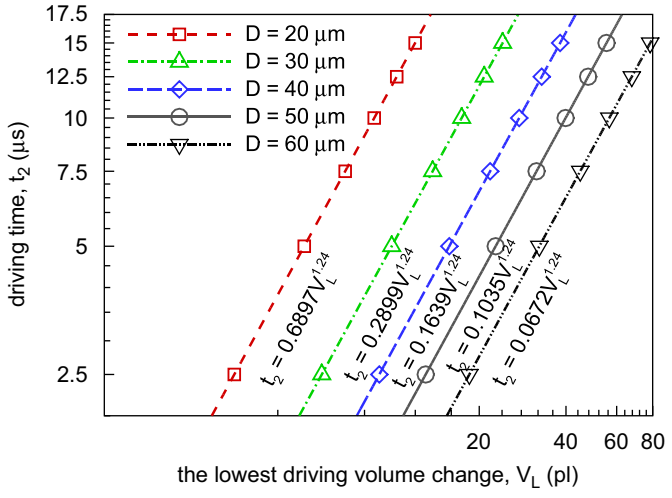

Fig. 5. Driving time versus the lowest driving volume.

associated with the driving time (t_2) and the nozzle diameter (D). Moreover, the lowest driving volume change (V_L) increased with the nozzle diameter (D) at the specific driving time (t_2) with relationship:

$$\frac{V_L^{1.24}}{t_2} = constant. \quad (4)$$

The nozzle diameter has a strong influence on the DOD PZT droplet generator. The promising range of the driving condition is widespread with the different nozzle diameters. Besides the lowest driving condition, we also identified the highest driving condition in which a liquid jet instead of a droplet would be ejected. The simulation results for the driving time of 10 μs are summarized in Fig. 6. The lowest driving volume change and the highest driving volume change were proportional to the square of the nozzle diameter. Here, we defined V/D^2 as a volume factor. From the physical point of view, V/D^2 is related to the length of the ejected droplet. Fig. 6 clearly marks the region of liquid jet ejection (upper left), no droplet ejection (lower right), and the region for droplet generation (middle). Volume factor V/D^2 is an important factor in this study when we discuss the influence of the driving conditions.

3.1.2. The driving conditions affecting the droplet velocity

Fig. 6 shows that the volume factor (V/D^2) defines an operation region beyond which no droplet will be ejected. Further analysis illustrates that the correlation between droplet velocity (S_d) and volume factor (V/D^2) had a linear relationship of a slope of 0.3422, as shown in Fig. 7 and could be expressed as

$$S_d = 0.3422\frac{V}{D^2} + constant. \quad (5)$$

Therefore, the droplets could have the same velocity (S_d) at different nozzle diameters as long as keeping the same volume factor (V/D^2). As for the effects of the driving time (t_2), we summarized the relationship between the droplet

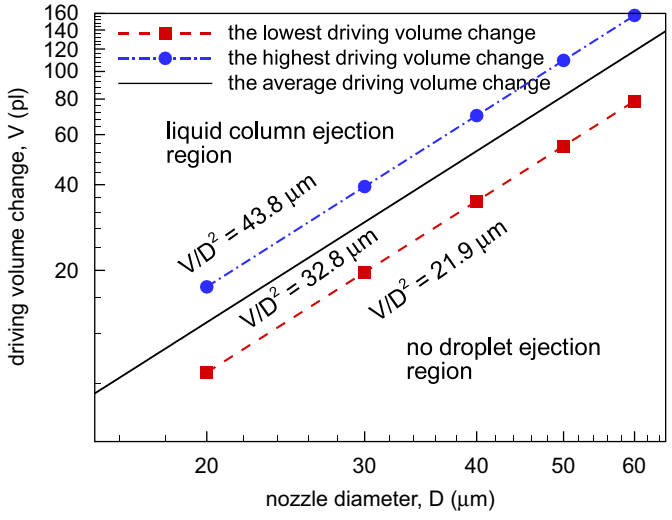

Fig. 6. Driving volume change versus nozzle diameter at $t_2 = 10$ μs.

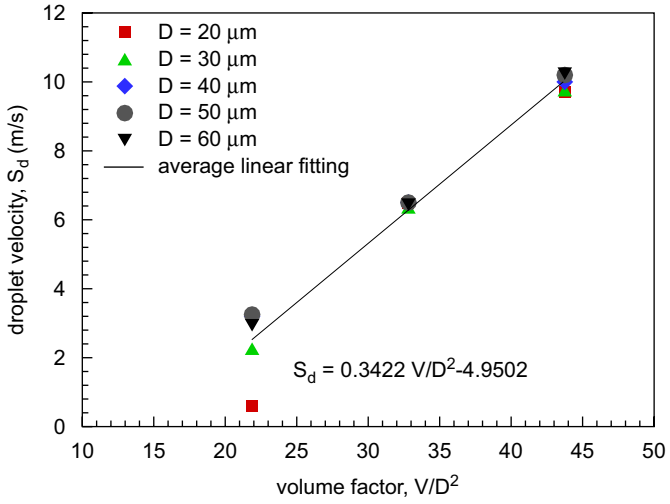

Fig. 7. Droplet velocity versus volume factor for nozzle diameter from 20 to 60 μm at $t_2 = 10$ μs.

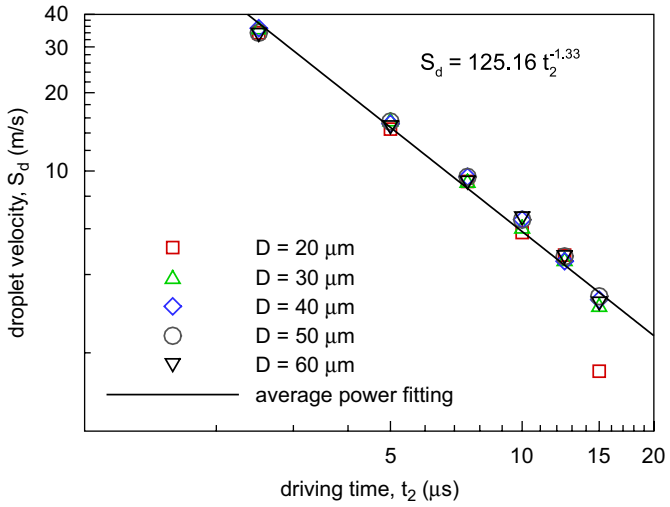

Fig. 8. Droplet velocity versus driving time for nozzle diameter from 20 to 60 μm, at $V/D^2 = 32.8$ μm.

velocity and the driving time in Fig. 8. The shorter driving time meant the faster driving velocity of the PZT and it resulted in the higher droplet velocity. In this case, regardless of the nozzle diameter, with the same value of volume factor (V/D^2) of 32.8 μm, the droplet velocity and the driving time had the following relationship:

$$S_d = 125.16 \cdot t_2^{-1.33}. \quad (6)$$

3.1.3. The volume factor affecting the droplet volume

The volume factor (V/D^2) is linearly proportional to the droplet volume. If the value of the volume factor does not change, a different nozzle diameter could have a different droplet volume as shown in Fig. 9. Under the same quantity of the volume factor, the relationship between the droplet volume and the nozzle diameter is

$$V_d \propto D^{2.5666}. \quad (7)$$

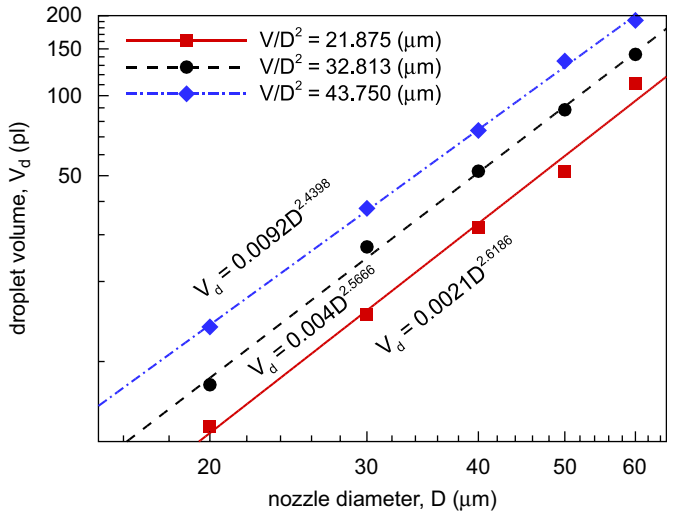

Fig. 9. Droplet volume versus nozzle diameter with the same volume factors at $t_2 = 10\,\mu s$.

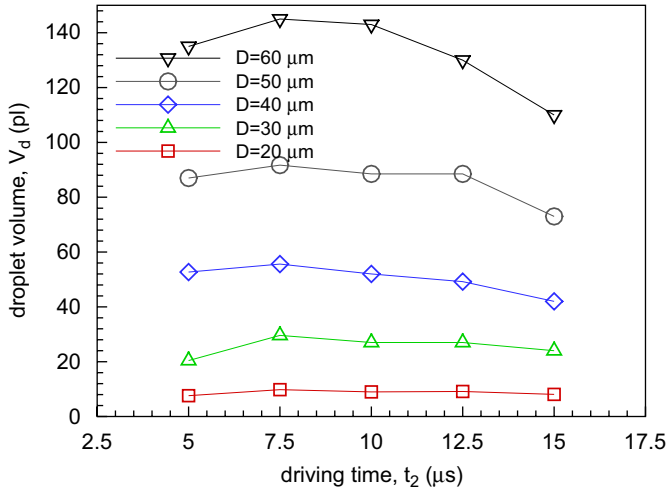

Fig. 11. The droplet volume versus driving time for nozzle diameter from 20 to 60 μm, at $D_t = 40\,\mu m$, $W = 200\,\mu m$, $H = 200\,\mu m$ and $V/D^2 = 32.8\,\mu m$.

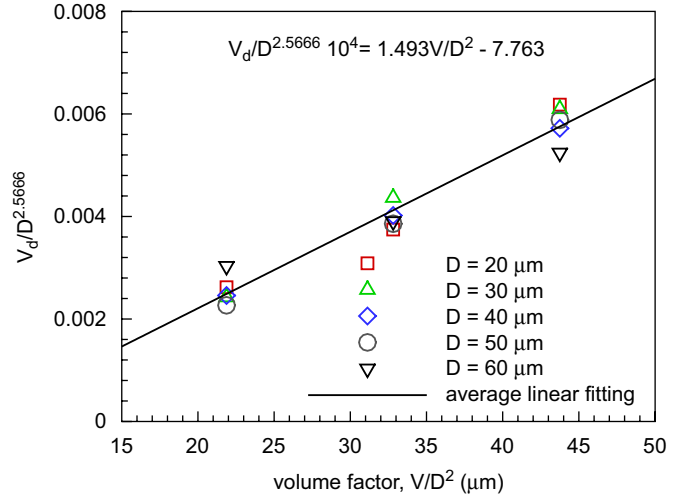

Fig. 10. The driving parameter, $V_d/D^{2.5666}$ versus V_d/D^2 for all nozzle diameters at $t_2 = 10\,\mu s$.

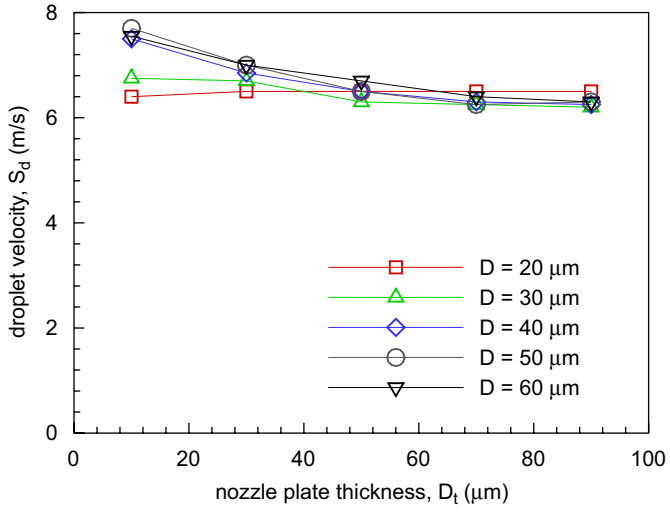

Fig. 12. The droplet velocity versus the nozzle plate thickness for nozzle diameters from 20 to 60 μm, at $W = 200\,\mu m$, $H = 200\,\mu m$, $V/D^2 = 32.8\,\mu m$ and $t_2 = 10\,\mu s$.

Therefore, the relationship between $V_d/D^{2.5666}$ and the volume factor (V/D^2) shown in Fig. 10 leads to the correlation formula:

$$\frac{V_d}{D^{2.5666}} = 0.0001493\frac{V}{D^2} - 0.0007763. \quad (8)$$

The influence of the driving time on the droplet volume is shown in Fig. 11. Fig. 11 shows that when the nozzle diameter was selected, a relatively smaller droplet was produced at the longer driving time. The droplet volume varied by 25% from the smallest to the largest. This characteristic was also exhibited in the previous experimental work [12].

3.2. Geometry effects

The influence of the geometrical dimensions such as the nozzle plate thickness (D_t), chamber depth (H) and width (W) at the same driving conditions is discussed here. The driving conditions were fixed at $t_2 = 10\,\mu s$, and $V/D^2 = 32.8\,\mu m$. The increasing thickness of the nozzle plate, which would increase the resistance of the fluid passage, affected the droplet velocity and the droplet volume. When $D_t/D \geqslant 1$, Fig. 12 shows that the influence of the nozzle plate thickness on the droplet velocity can be ignored. In Fig. 13, the variation of the droplet volume was about 8% due to the different nozzle plate thickness.

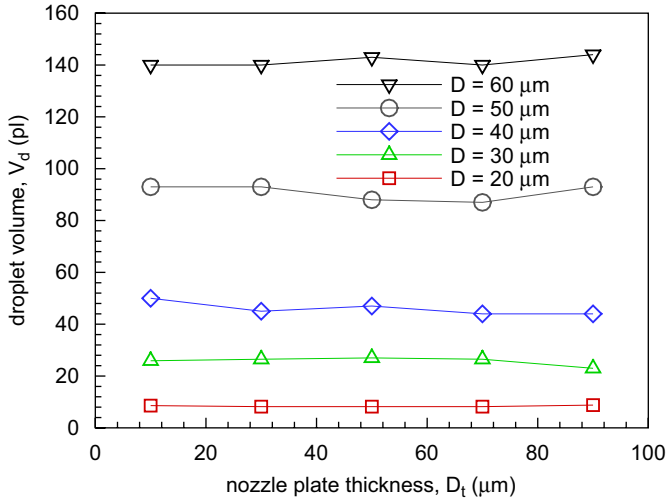

Fig. 13. The droplet volume versus the nozzle plate thickness for nozzle diameters from 20 to 60 μm, at $W = 200\,\mu m$, $H = 200\,\mu m$, $V/D^2 = 32.8\,\mu m$ and $t_2 = 10\,\mu s$.

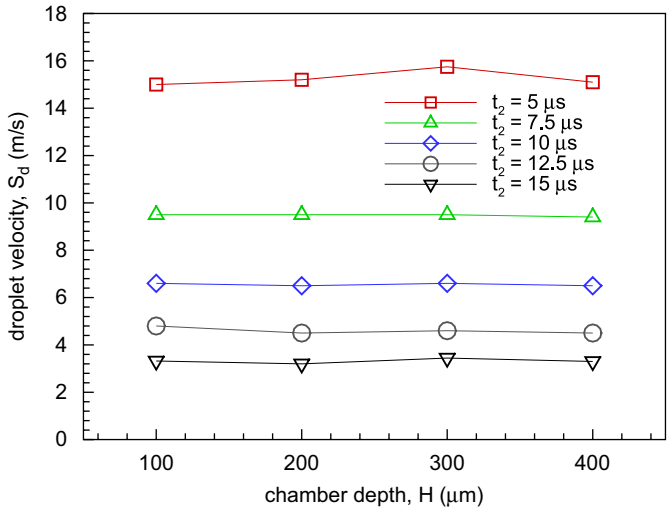

Fig. 14. Droplet velocity versus chamber depth for the driving time from 5 to 15 μs, at $D = 40\,\mu m$, $W = 200\,\mu m$, $D_t = 50\,\mu m$, $V/D^2 = 32.8\,\mu m$ and $t_2 = 10\,\mu s$.

The influence of the chamber depth is shown in Figs. 14 and 15. The influence of the chamber depth on the droplet velocity was limited. The influence of the chamber width varied from $W = 200$ to $400\,\mu m$ was 3% for droplet velocity and 7% for droplet volume.

4. Conclusion

This paper investigated the influence of design parameters of a DOD PZT droplet generator. The simplified 2-D axisymmetric approach had been adopted for the analysis. The previous experimental data were first used to verify our simulation results with error of 6.2%. The influence of design parameters, such as nozzle diameter, chamber width and chamber depth, as well as the driving

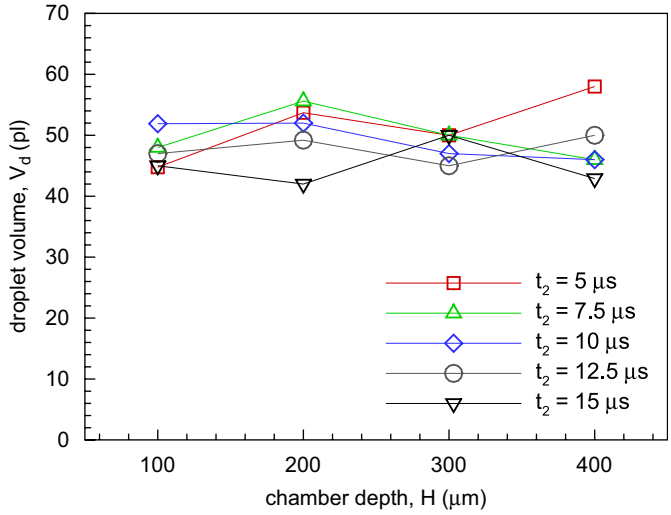

Fig. 15. Droplet volume versus chamber depth for the driving time from 5 to 15 μs, at $D = 40\,\mu m$, $W = 200\,\mu m$, $D_t = 50\,\mu m$, $V/D^2 = 32.8\,\mu m$ and $t_2 = 10\,\mu s$.

conditions on droplet volume and droplet velocity was presented. Two empirical formulas, Eqs. (5) and (8), were derived based on the simulation data. Eq. (5) enables to define the driving volume change and the nozzle diameter to achieve the desired droplet velocity. Eq. (8) allows defining the driving volume and the nozzle diameter to eject droplet at a desired droplet volume. Based on the results, when $D_t/D \geqslant 1$, the influence of the nozzle plate thickness on the droplet velocity could be ignored. The variation of the droplet volume was about 8% in the different nozzle plate thickness. The influence of the chamber depth on the droplet velocity is limited. Finally, the influence of the chamber width was 3% for droplet velocity and 7% for droplet volume. The above summary is based on the specified geometry discussed in the text.

In summary, the presented formula and figures provide an easy-to-use tool for the design of the DOD PZT droplet generator. For instance, we desire to design a droplet generator with a specified droplet velocity (S_d), so that we could easily find the corresponding design parameters, such as V/D^2 from Fig. 7, t_2 from Fig. 8, D from Figs. 6 and 7, V from Fig. 6, V_L from Fig. 5, V_d from Fig. 9, D_t from Fig. 12, and H from Fig. 14. Finally, for the specified droplet volume we could use Fig. 10 to find V and D, and find D_t and H from Figs. 13 and 15.

Acknowledgments

Financial support by the Nation Science Council under the project numbers of NSC-92-2212-E-002-089 and NSC-93-2212-E002-074 are deeply appreciated.

References

[1] Cooley P, Wallace D, Antohe B. Applications of ink-jet printing technology to BioMEMS and microfluidic systems. Proceedings of

the Society of Photo-Optical Instrumentation Engineers 2001;4560: 177–88.
[2] Rose D. Microdispensing technologies in drug discovery. Drug Discovery Today 1999;4(9):411–9.
[3] Hayes DJ, Wallace DB, Cox WR. Microjet printing of solder and polymers for multi-chip modules and chip-scale packages. IMAPS, MicroFab Technologies, Inc. 1999. p. 1–5.
[4] Cox WR, Guan C, Hayes DJ, Wallace DB. Microjet printing of micro-optical interconnects. International Journal of Microcircuits and Electronic Packaging 2000;23(3):346–51.
[5] Hebner TR, Wu CC, Marcy D, Lu MH, Sturm JC. Ink-jet printing of doped polymers for organic light emitting devices. Applied Physics Letters 1998;72(5):519–21.
[6] Chang S, Bharathan J, Yang Y, Helgeson R, Wudl F, Ramey MB, Reynolds JR. Dual-color polymer light-emitting pixels processed by hybrid inkjet printing. American Institute of Physics 1998;73(18): 2561–3.
[7] Percin G, Butrus TKY. Piezoelectric droplet ejector for ink-jet printing of fluids and solid particles. Review of Scientific Instruments 2003;74(2):1120–7.
[8] Fromm JE. Numerical calculation of the fluid dynamics of drop-on-demand jets. IBM Journal of Research and Development 1984;28(3): 322–33.
[9] Yeh JT. A VOF-FEM and coupled inkjet simulation. In: Proceedings of ASME FEDSM, New Orleans, USA; 2001. p. 1–5.
[10] Shin DY, Grassia P, Derby B. Numerical and experimental comparisons of mass transport rate in a piezoelectric drop-on-demand inkjet print head. International Journal of Mechanical Sciences 2004;46:181–99.
[11] Liou TM, Chan CY. Three-dimensional coupled piezoelectric-structural-fluid simulations of inkjet flows. The First International Symposium on Micro & Nano Technology, Honolulu Hawaii, USA; 2004. p. 1–6.
[12] Chen PH, Peng HY, Liu HY, Chang SH, Wu TI, Cheng CH. Pressure response and droplet ejection of a piezoelectric inkjet printhead. International Journal of Mechanical Sciences 1999;41: 235–48.
[13] Hirt CW, Nichols BD. Volume of fluid (VOF) method for the dynamics of free boundaries. Journal of Computational Physics 1981; 39(1):201–25.
[14] Coventorware Version 2003: Analyzer tutorials, Coventor, Inc., Cary, NC, 2003. F6-1-F6-40.
[15] Van Doormaal JP, Raithby GD. Enhancement of the SIMPLE method for predicting incompressible fluid flows. Numerical Heat Transfer 1984;7:147–63.